Regulation of ciliary polarity by the APC/C

Athina Ganner[a,1], Soeren Lienkamp[a,1], Tobias Schäfer[a,1], Daniel Romaker[a], Tomasz Wegierski[a], Tae Joo Park[b], Stefan Spreitzer[a], Matias Simons[a], Joachim Gloy[a], Emily Kim[a], John B. Wallingford[b], and Gerd Walz[a,2]

[a]Renal Division, Department of Medicine, University Hospital Freiburg, Hugstetter Strasse 55, 79106 Freiburg, Germany; and [b]Molecular Cell and Developmental Biology and Institute for Cellular and Molecular Biology, University of Texas, Austin, TX 78712

Edited by Kathryn V. Anderson, Sloan–Kettering Institute, New York, NY, and approved August 31, 2009 (received for review August 20, 2009)

Planar cell polarity signaling controls a variety of polarized cell behaviors. In multiciliated *Xenopus* epidermal cells, recruitment of Dishevelled (Dvl) to the basal body and its localization to the center of the ciliary rootlet are required to correctly position the motile cilia. We now report that the anaphase-promoting complex (APC/C) recognizes a D-box motif of Dvl and ubiquitylates Dvl on a highly conserved lysine residue. Inhibition of APC/C function by knockdown of the ANAPC2 subunit disrupts the polarity of motile cilia and alters the directionality of the fluid movement along the epidermis of the *Xenopus* embryo. Our results suggest that the APC/C activity enables cilia to correctly polarize in *Xenopus* epidermal cells.

cilium | Dishevelled | planar cell polarity | polycystic kidney disease | ANAPC2

Dishevelled (Dvl) is a central component of the Wnt signaling cascade. In canonical Wnt signaling, binding of soluble Wnts to the cysteine-rich domains of Frizzled receptors triggers the association with low-density-lipoprotein coreceptors and the recruitment of Axin and Dvl to the heteromeric receptor complex. Recruitment of Axin to low-density-lipoprotein coreceptors and phosphorylation of Dvl stabilize cytosolic β-catenin, which translocates to the nucleus and forms a complex with transcription factors of the lymphoid enhancer-binding factor/T cell-specific factor (LEF/TCF) family to activate gene expression. In noncanonical β-catenin-independent Wnt signaling, the Frizzled/Dvl complex initiates the asymmetric accumulation of core planar cell polarity (PCP) proteins such as Flamingo/Starry Night (Fmi/Stan), Strabismus/Van Gogh (Stbm/Vang), Prickle (Pk), and Diego (Dgo). In the *Drosophila* wing, Frizzled, Dvl, and Dgo move to the distal side of the cell, whereas Pk and Stbm accumulate at the proximal plasma membrane. Planar cell polarity effectors such as Inturned (In), Fuzzy (Fy), and RhoA then organize the cytoskeleton and orient cells and their appendages in the plane of the tissue (reviewed in refs. 1 and 2). Interaction between Frizzled and Dvl is a prerequisite for PCP signaling (3); however, subsequent stabilization of the Frizzled/Dvl complex by components of the PCP complex, such as the protein Dgo, is necessary to maintain the Frizzled/Dvl complex at the plasma membrane (4).

Recent findings have uncovered a crucial role of Dvl in the apical docking of basal bodies and subsequent polarization of the motile cilia on the *Xenopus* epidermis (5). These cilia produce a flow along the anterior-to-posterior axis of the *Xenopus* embryo during gastrulation. Dvl is asymmetrically localized at the base of the cilia; this asymmetry is required to polarize the cilia and direct the fluid flow. Stabilization or degradation are thought to promote the asymmetric distribution of Dvl at the basal body; however, the underlying molecular mechanisms are currently unknown.

Several ubiquitin ligases control mammalian Dvl localization and turnover. The HECT-type ubiquitin ligase NEDL1 ubiquitylates Dvl1 (6), whereas the KLHL12–Cullin-3 ubiquitin ligase targets Dvl3 for degradation (7). Wnt modulators such as Naked cuticle/PR72 and Prickle1 appear to regulate Dvl levels through interaction with ubiquitin ligases (8, 9), whereas Dapper 1 seems to target Dvl for lysosomal degradation (10). Inversin, an ankyrin-repeat protein related to the PCP proteins Diversin and *Drosophila* Dgo, interacts with Dvl and targets cytoplasmic Dvl for ubiquitin-dependent degradation (11). Because Inversin interacts with ANAPC2 (12), a cullin-domain-containing subunit of the anaphase-promoting complex/cyclosome (APC/C), this observation suggests that Inversin uses the APC/C to target Dvl for degradation.

The APC/C is a multisubunit protein complex with at least 12 core subunits and several coactivators that regulate eukaryotic cell cycle progression (reviewed in ref. 13). During mitosis, components of the spindle-assembly checkpoint, such as Mad1, Mad2, Mad3/BubR1, Bub1, and Bub3, prevent Cdc20 from activating APC/C to ensure the fidelity of chromosome segregation (14). Other inhibitors of the APC/C, such as members of the Emi family, function as pseudosubstrates to inhibit the APC/C (reviewed in ref. 15). After phosphorylation by calmodulin kinase II (CaMKII) and polo kinase 1 (Plk1/Plx1), these inhibitors are recognized by the β-TrCP E3 ubiquitin ligase and targeted for degradation by the 26S proteasome. Cell-cycle-independent functions of the APC/C are increasingly appreciated (reviewed in refs. 13 and 16). The APC/C is involved with the control of axon growth and brain patterning (17), regulates synaptic size and activity in *Caenorhabditis elegans* and *Drosophila* (18, 19), and excludes Par-3 from the posterior cortex of the *C. elegans* embryo to establish its anterior–posterior axis (20). The APC/C is needed to asymmetrically localize Miranda and its cargo proteins Staufen, Prospero, and Brat during *Drosophila* neuroblast division, indicating a role for the APC/C in PCP (21).

We now report that expression of the APC/C subunit ANAPC2 activates the APC/C-dependent degradation of Dvl by disrupting canonical Wnt signaling. Knockdown of ANAPC2 in *Xenopus* embryos impaired the polarization of motile cilia of the *Xenopus* epidermis, demonstrating that APC/C activity is required to establish a directed fluid flow.

Results

Expression of ANAPC2 Targets Dvl for Ubiquitin-Dependent Degradation. We observed that expression of ANAPC2 reduced both transiently expressed murine Dvl1 and endogenous Dvl in HEK 293T cells (Fig. 1*A*). Purification of a Flag-His-tagged version of Dvl1 under denaturing conditions revealed its increased polyubiquitylation in the presence of ANAPC2 (Fig. 1 *B* and *C*). Furthermore, ANAPC2 increased turnover of Dvl1 (Fig. 1*D*). ALLN, a proteasome inhibitor, prevented the degradation of Dvl1 (Fig. 1*E*). To demonstrate that the ANAPC2-induced degradation of Dvl1 engages the APC/C, we used established modulators of APC/C activity. The *Xenopus* Emi1-related pro-

Author contributions: A.G., S.L., T.S., M.S., J.G., and G.W. designed research; A.G., S.L., T.S., D.R., T.W., T.J.P., S.S., and M.S. performed research; A.G., S.L., T.S., T.W., T.J.P., J.G., J.B.W., and G.W. analyzed data; and E.K. and G.W. wrote the paper.

The authors declare no conflict of interest.

This article is a PNAS Direct Submission.

[1]A.G., S.L., and T.S. contributed equally to this work.

[2]To whom correspondence should be addressed. E-mail: gerd.walz@uniklinik-freiburg.de.

This article contains supporting information online at www.pnas.org/cgi/content/full/0909465106/DCSupplemental.

DEVELOPMENTAL BIOLOGY

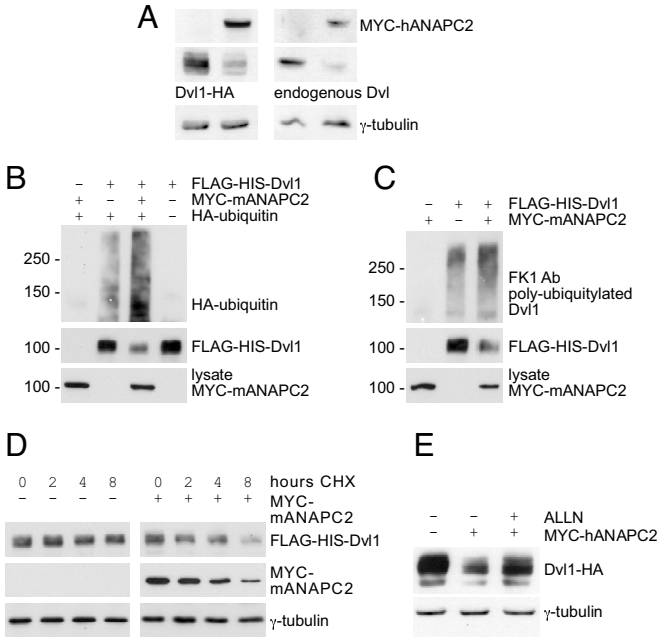

Fig. 1. ANAPC2 targets Dvl for ubiquitin-dependent degradation. (*A*) Levels of both transiently expressed (*Left*) and endogenous Dvl (*Right*) were reduced in HEK 293T cells expressing ANAPC2; γ-tubulin levels were used as a loading control. (*B*) Expression of Myc-tagged ANAPC2 led to an increase in ubiquitiylated Dvl in HEK 293T cells, cotransfected with Flag-His-tagged Dvl1 and HA-tagged ubiquitin. (*C*) Coexpression with Myc-ANAPC2 enhanced the conjugation of endogenous ubiquitin to Dvl1, as detected by the polyubiquitin antibody FK1. (*D*) The half-life of Dvl1 decreased in the presence of ANAPC2. Forty-eight hours after the transfection of HEK 293T cells, 40 μg·mL^{-1} cycloheximide (CHX) was added for 0, 2, 4, and 8 h. The levels of Dvl1 and Myc-ANAPC2 were monitored by Western blot analysis, and γ-tubulin levels were used as a loading control. (*E*) The proteasome inhibitor ALLN (30 μM) reversed the ANAPC2-mediated reduction of Dvl1 levels; γ-tubulin levels were used as a loading control.

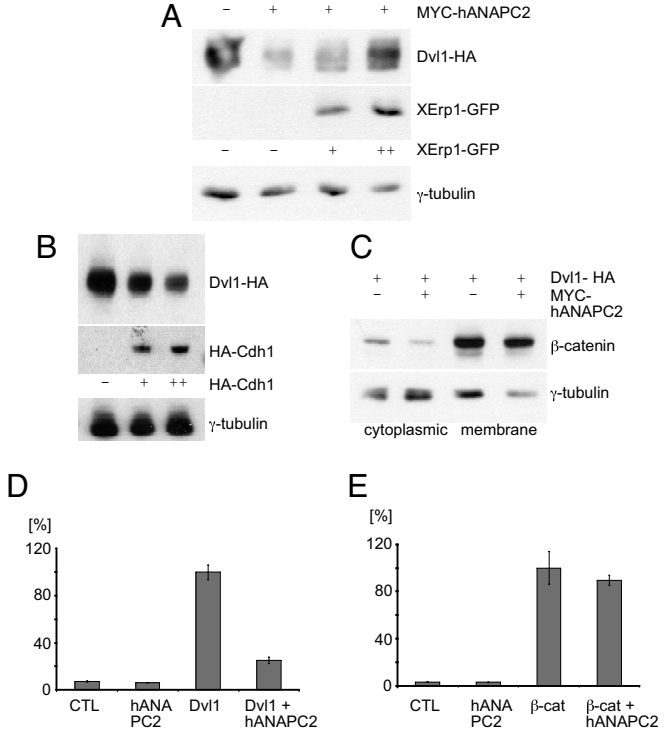

Fig. 2. ANAPC2 inhibits canonical Wnt signaling. (*A*) In HEK 293T cells, the APC/C inhibitor XErp1 reversed the ANAPC2-dependent reduction of Dvl1 levels in a dose-dependent manner; γ-tubulin levels were used as a loading control. (*B*) The APC/C activator Cdh1 reduced Dvl1 levels in a dose-dependent manner. (*C*) Expression of ANAPC2 reduced levels of cytosolic but not membrane-bound endogenous β-catenin in HEK 293T cells cotransfected with Dvl1-HA; γ-tubulin served as a loading control. (*D*) ANAPC2 inhibited Dvl1-induced activation of the TOPFLASH reporter construct in transiently transfected HEK 293T cells. (*E*) ANAPC2 had no effect on β-catenin-induced activation of the TOPFLASH reporter construct in transiently transfected HEK 293T cells.

tein 1 (XErp1), a pseudosubstrate inhibitor of the APC/C during meiosis (22), blocked the ANAPC2-mediated decrease of Dvl1 steady-state levels (Fig. 2*A*), whereas the APC/C activator Cdh1 facilitated degradation of Dvl1 (Fig. 2*B*). Together, these data suggest that expression of ANAPC2 activates the APC/C to stimulate degradation of cytoplasmic Dvl in HEK 293T cells.

The APC/C Antagonizes Canonical Wnt Signaling. To determine the consequences of APC/C-induced Dvl degradation, we examined cytoplasmic β-catenin levels in cells coexpressing ANAPC2. A reduction in cytoplasmic β-catenin levels was observed in HEK 293T cells expressing ANAPC2 (Fig. 2*C*), suggesting that ANAPC2 antagonizes canonical Wnt signaling. The function of ANAPC2 was further characterized using TOPFLASH reporter assays. ANAPC2 reduced Dvl1-mediated but not β-catenin-mediated activation of TCF-dependent transcription (Fig. 2 *D* and *E*), showing that ANAPC2 inhibits Wnt target gene activation upstream of β-catenin. To examine ANAPC2-mediated Dvl degradation in vivo, we activated the canonical Wnt pathway during *Xenopus* embryogenesis. ANAPC2 blocked secondary axes induced by *Xenopus* Dvl2 mRNA (Fig. 3*A*) but had no effect on TCF3 mRNA-mediated axis duplication. (Fig. 3*B*), confirming that ANAPC2 blocks the canonical Wnt signal pathway at the level of Dvl in vivo. Together, these data confirm that activation of APC/C through ectopic expression of ANAPC2 targets Dvl for degradation, interfering with canonical Wnt signaling in vitro and in vivo.

The APC/C Targets a Conserved D-Box of Dvl. Substrate recognition by the APC/C occurs through a variety of degradation motifs, the most common of which are the destruction box (D-box) and the KEN-box. Sequence analysis of murine Dvl1 revealed three potential destruction boxes containing the RxxL consensus motif, located in the N or C terminus (Fig. 4*A*). To determine whether the D-boxes regulate Dvl1 stability, we examined the protein levels of two murine Dvl1 truncations in the presence of ANAPC2. An N-terminal deletion lacking the first two D-boxes (mDvl1ΔDIX) was degraded in the presence of ANAPC2. However, a C-terminal deletion mutant lacking the DEP domain (mDvl1ΔDEP) remained stable despite coexpression of ANAPC2 (Fig. 4*B*), suggesting that the APC/C recognizes the highly conserved D-box 3 (Fig. 4*A*). To confirm this, a Dvl1 RxxL → AxxA mutant was tested in HEK 293T cells. Mutation of the third D-box increased Dvl1 steady-state levels in the presence of ANAPC2 (Fig. 4 *C* and *D*). Thus, the RxxL motif present in the DEP domain mediates the ANAPC2-dependent ubiquitylation and degradation of Dvl. To demonstrate that APC/C-mediated degradation of Dvl requires D-box 3 in vivo, we compared the phenotypic effect of wild-type and mutant Dvl1 by using double-axis formation in *Xenopus*. The more stable AxxA Dvl1 mutant induced an increase in secondary body axis formation during *Xenopus* embryogenesis compared with that of wild-type protein (Fig. 4*E*). These findings support our hypothesis that APC/C controls the half-life of Dvl in vivo. Typically, one or more lysine residues serve as ubiquitin attachment sites (reviewed in ref. 23), so our suspicions fell upon a highly

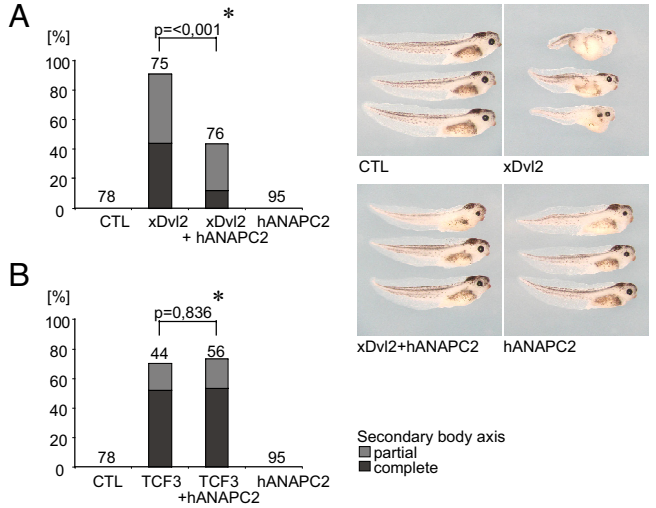

Fig. 3. ANAPC2 inhibits the formation of a secondary body axis in *Xenopus* embryos. (*A*) Four-cell-stage embryos were injected with mRNA into one ventral blastomere and scored at the tadpole stage. The secondary body axis induced by xDvl2 (0.5 ng) was rescued by ANAPC2 (1.0 ng), whereas ANAPC2 itself had no effect on the formation of secondary body axes. (*B*) The secondary body axis induced by TCF3-VP16 (4 pg) was not affected by ANAPC2. A partial secondary axis consists of a secondary trunk and tail only, whereas a complete secondary axis also includes duplicated head structures such as eyes and the cement gland. Numbers above bars represent the injected embryos. The *P* value (*) was calculated by the Mann–Whitney rank sum test.

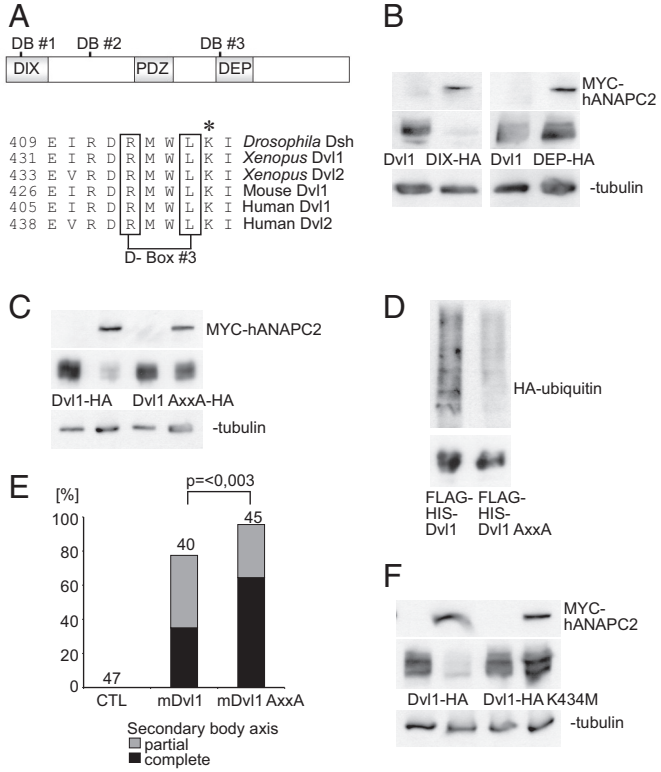

Fig. 4. Degradation of Dvl by ANAPC2 depends on a conserved D-box within the DEP domain. (*A*) Schematic representation of mouse Dvl1 indicating the three potential D-boxes and the DIX, PDZ, and DEP domains of the protein. Alignment of the amino acid sequence of *Drosophila*, *Xenopus*, mouse, and human Dvl flanking the third D-box. The asterisk (*) denotes a conserved lysine residue immediately adjacent to the third D-box. (*B*) APC2 reduced the protein levels of a mutant mouse Dvl1 that lacks the first two D-boxes (Dvl1ΔDIX-HA) but had no effect on a mouse Dvl1 construct missing the third D-box (Dvl1ΔDEP-HA). (*C*) Mutation of D-box 3, replacing the RxxL motif by AxxA, protected Dvl1 against the effects of ANAPC2; γ-tubulin served as a loading control. (*D*) Ubiquitylation of a Flag-His-tagged Dvl1 mutant (Flag-His-Dvl1 AxxA) is reduced compared with Flag His-tagged wild-type Dvl1 (Flag-His-Dvl1). With a nickel column, the His-tagged proteins were isolated under denaturing conditions from transiently transfected HEK 293T cells coexpressing HA-tagged ubiquitin. (*Upper*) Incorporation of HA-ubiquitin. (*Lower*) Demonstration of the precipitated Dvl1 proteins, using an anti-Flag antibody. (*E*) As a consequence of its increased stability, mouse Dvl1 AxxA induces more secondary body axes in *Xenopus* embryos compared with the wild-type protein ($P < 0.003$, Mann–Whitney rank sum test). (*F*) The lysine at position 434 in mouse Dvl1 is critical for ANAPC2-dependent degradation of Dvl1 levels. In transfected HEK 293T cells, a Dvl1 K434M mutation is not targeted by ANAPC2.

conserved lysine that lies adjacent to the third D-box (Fig. 4*A*). Indeed, ANAPC2 failed to diminish levels of Dvl1 when the critical lysine was replaced by methionine (Fig. 4*F*), indicating that this residue mediates APC2-dependent ubiquitin attachment. Interestingly, two *Drosophila* Dvl mutations (dsh^{A3} and dsh^{1}) that specifically affect PCP signaling (24–27) map to either the third D-box (R413H) or the adjacent lysine (K417M).

APC/C Activity Is Required To Polarize the Motile Cilia of the *Xenopus* Epidermis. To analyze a possible function for ANAPC2-mediated Dvl degradation, morpholino oligonucleotides (MOs) targeting the splice sites of the intron/exon boundaries of ANAPC2 intron 2 were used (Fig. 5*A*). This approach delayed the onset of ANAPC2 depletion, avoiding early cytotoxicity. Fate maps were used to selectively target the MO to defined tissues (28). ANAPC2 MO or ANAPC2 RNA injection, directed to the dorsal blastomeres, resulted in classical axis elongation and neural tube closure defects, which were identical to the changes described for Dvl depletion or overexpresssion (29). The phenotype caused by depletion of ANAPC2 was partially rescued by coinjection of murine APC2 RNA not targeted by the MO, indicating that the observed phenotype was specific to ANAPC2 depletion (Fig. S1).

In multiciliated cells of the *Xenopus* epidermis, Dvl is required to dock the basal bodies to the apical membrane, which precedes the nucleation of the ciliary axoneme (5). In completely polarized cilia, Dvl is confined to the center of the ciliary rootlet immediately adjacent to the basal body; this asymmetric Dvl localization was shown to maintain the polarization of motile cilia of the *Xenopus* epidermis (5). Immunostaining of human respiratory epithelial cells revieled a localization of both Dvl and ANAPC2 at the basal body region (Fig. S2).

In addition, the MO concentrations were titrated to allow normal embryonic development and epidermal differentiation (Fig. S1). We found that two nonoverlaping MO, targeted to the *Xenopus* epidermis, randomized the localization of the ciliary rootlet in relationship to the basal body, marked by CLAMP-GFP and Centrin-red fluorescent protein (RFP), respectively (Fig. 5*B*). Knockdown of *Xenopus* ANAPC2 also reduced the speed of particles moving across the *Xenopus* epidermis (Fig. 5*C*), suggesting that the APC/C is required to maintain the polarization of motile cilia.

To investigate whether the APC/C affects the localization of Dvl, we expressed very low levels of xDvl2-GFP (50 pg). At this dose, no developmental alterations were observed, and the Dvl2-GFP signal was barely detectable along the plasma membrane. When ANPAC2 MO was coinjected, Dvl2-GFP aggregates became readily detectable. Some aggregates showed a randomized polarization relative to the basal body; others were not associated with basal bodies at all (Fig. 5*D*). To exclude an unspecific accumulation of GFP, membrane-tagged GFP (mem-GFP) was used as a control (Fig. S3). To demonstrate that xDvl2-GFP is targeted by ANAC2 in vivo, we analyzed *Xenopus* lysates expressing xDvl2-GFP in combination with or without

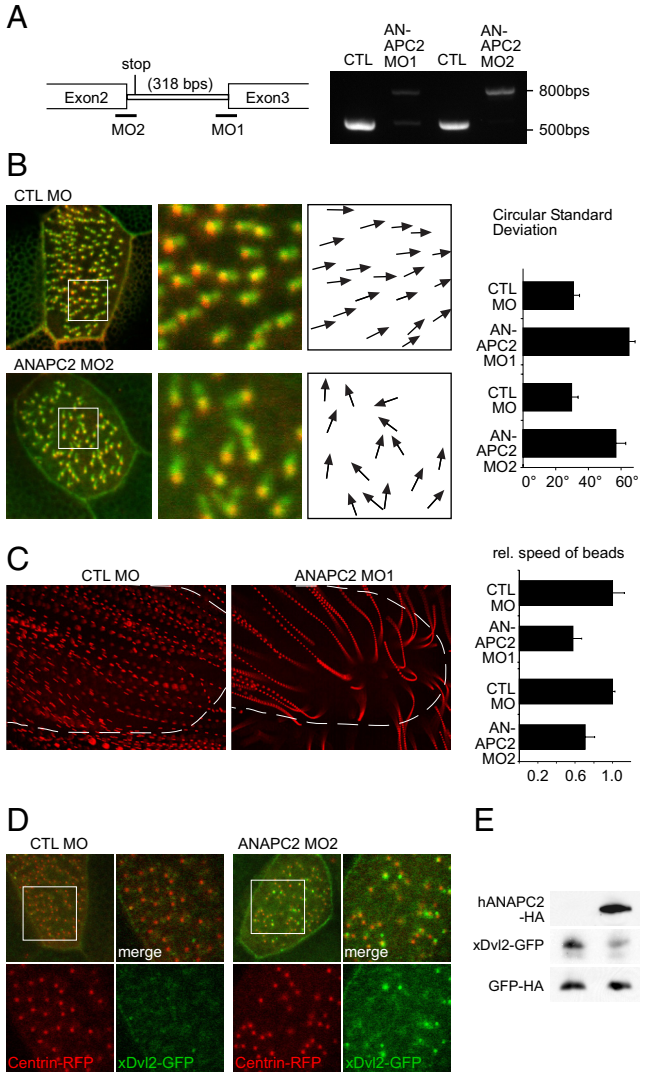

Fig. 5. Depletion of ANAPC2 causes ciliary polarity defects. (*A*) The efficiency of two nonoverlapping, splice-blocking ANAPC2 MOs was monitored by RT-PCR. (*B*) The two MOs were injected into the ventral blastomeres to preferentially target the APC/C activity in the *Xenopus* epidermis. Depletion of *Xenopus* ANAPC2 caused a randomization of the position of the rootlet, labeled by CLAMP-GFP, in relationship to the basal body, marked by Centrin-RFP. The polarization was quantified by angular measurements of all CLAMP/Centrin pairs in 10 cells; white boxes show the magnified areas, and arrows indicate the direction of the ciliary rootlet in relation to its basal body. Depletion of ANAPC2 by either ANAPC2 MO increased the circular standard deviation compared with that of controls ($P < 0.001$; error bars represent SEM, $n = 10$). (*C*) The randomized polarization of the motile cilia resulted in a significantly reduced speed of fluorescent particles applied to the *Xenopus* epidermis. Single particles, tracked by Imaris 6.0 software, were depicted as streamlines after superimposing the single frames of video recordings. Broken lines depicted the positions of the embryos. Because of the decreased speed, the streamlines of ANAPC2-MO-injected tadpoles are more punctuated, and the distances between individual dots are smaller ($P < 0.05$; error bars represent SEM, $n > 10$). In addition, some particles showed disordered movements and circular trajectories toward the end of the tracked movements. (*D*) Low levels of xDvl2-GFP (50 pg) were coexpressed with Centrin-RFP (200 pg) in epidermal ciliated cells. Larger magnifications of the boxed area are at right. Channels are separated. In embryos injected with the control (CTL) MO, the xDvl2-GFP signal was barely detectable, whereas xDvl2-GFP formed visible aggregates in *Xenopus* embryos coinjected with ANAPC2 MO. (*E*) In whole-embryo lysates, overexpression of human ANAPC2 reduced the steady-state levels of xDvl2-GFP. The RNA coding for xDvl2-GFP and HA-tagged GFP were coinjected without (*Left*) or with ANAPC2 mRNA (*Right*) into four-cell-stage embryos. Embryo lysates were prepared at stage 10.5 and analyzed for protein levels by Western blot. Although ANAPC2 reduced xDvl2-GFP levels, the levels of GFP remained unaffected by ANAPC2.

ANAPC2. As shown in Fig. 5*E*, ANAPC2 decreased the steady-state levels of xDvl2-GFP in microinjected embryos.

Discussion

The ankyrin-repeat protein Inversin switches between canonical and noncanonical Wnt signaling by targeting cytosolic Dvl for ubiquitin-dependent degradation (11). Inversin interacts with the APC/C subunit ANAPC2 (12) and mediates the formation of a heterotrimeric complex with Dvl (11). ANAPC2 lies in close proximity to Cdh1 and together with ANAPC11 forms a platform at which substrates are ubiquitylated (30). Ectopic expression of ANAPC2 induces the ubiquitin-dependent degradation of Dvl. The APC/C appears to play a pivotal role: The APC/C inhibitor XErp1 blocks the ANAPC2-induced degradation of Dvl, whereas the APC/C activator Cdh1 facilitates Dvl degradation. Furthermore, Dvl degradation is contingent on the presence of a conserved D-box and an adjacent lysine residue within the DEP domain of Dvl; mutation of this D-box stabilizes Dvl and initiates canonical Wnt signaling and double-axis formation in the *Xenopus* embryo. Because we did not detect a direct interaction between Dvl and ANAPC2, adaptor proteins such as Inversin may link Dvl to ANAPC2 to initiate APC/C-dependent degradation. Although the tetratricopeptide repeat domain (TRP) domains of Cdc27/ANAPC3 and ANAPC7 are thought to interact with Cdh1 to recruit substrates to the proximity of the cullin/RING core formed by ANAPC2/ANAPC11 (31), Cdh1 appears capable of both direct and indirect interaction with ANAPC2 (32). Because both ANAPC2 and ANAPC11 can dissociate selectively from the APC/C (31), ANAPC2 conceivably recruits additional binding partners to the APC/C to initiate their degradation by this E3 ubiquitin ligase in nondividing cells.

Cell cycle-independent functions of the APC/C are well documented, but how the activity of the APC/C is regulated in interphase cells is largely unknown. The APC/C is present on centrosomes in dividing cells (33), suggesting that the centrosomal region harbors the APC/C activity required to control Dvl protein levels in *Xenopus* epidermal cells. Dvl orchestrates the functions of Rho, Inturned, and Sec8 to dock the basal bodies of budding cilia to the apical membrane. Dvl subsequently assumes an asymmetric localization within the center of the ciliary rootlet (5). Our findings reveal that the APC/C is essential for maintaining the Dvl-dependent polarity of these motile cilia. The initial polarization of the motile cilia of the *Xenopus* embryo is established by tissue patterning; however, subsequent refinement through fluid flow determines the final ciliary polarity (34). Because the cilia of the *Xenopus* epidermis function as both motile effectors and mechano-sensory organelles, mechano-sensory signaling such as flow-induced calcium transients may regulate the activity of the APC/C and thereby spatially modulate the degradation of Dvl that underlies the asymmetric accumulation of Dvl at the basal bodies of multiciliated *Xenopus* epidermal cells.

Another line of evidence to support the role of APC/C in cellular asymmetry and PCP signaling comes from a recent genetic screen for defective neuroblast division in *Drosophila*. The APC/C subunit ANAPC5 was identified as a crucial component of asymmetric Miranda localization (21). In PCP, gain-of-function and loss-of-function mutations often produce similar phenotypes, suggesting that the steady-state levels of PCP components are precisely controlled to maintain normal polarization and tissue asymmetry. Thus, a resistance to APC/C-mediated degradation could explain the PCP defects observed in the *Drosophila* Dsh^{1} and Dsh^{A3} mutants, insinuating a more general role for the APC/C in noncanonical Wnt signaling.

Materials and Methods

Reagents and Plasmids. ALLN (Sigma) and cycloheximide (Sigma) were used at concentrations as indicated. Human Myc-His-tagged ANAPC2 was provided by J. M. Peters (Research Institute of Molecular Pathology, Vienna), and mouse Myc-tagged ANAPC2 was provided by Y. Xiong (Lineberger Comprehensive Cancer Center, University of North Carolina, Chapel Hill). HA-tagged full-length Dvl, murine DvlHAΔDEP, and DvlHAΔDIX were provided by P. Salinas (Imperial College, London). XErp1-GFP was provided by T. U. Mayer, Max-Planck-Institute of Biochemistry, Martinsried, Germany, and plasmids for *Xenopus* Dvl2 (xDvl2, formerly *Xenopus* Dsh), β-catenin, and TCF3 (TCF3-VP16) were provided by S. Sokol (Mount Sinai School of Medicine, New York). Flag-His-tagged Dvl was generated by PCR using standard cloning techniques. HA-GSK3β, HA-ubiquitin, and M/P DvlHA, containing a myristylation/palmitoylation site, were described in ref. 11. DvlHA AxxA, xDvl2 AxxA, and DvlHA K to M were constructed by site-directed mutagenesis. Antibodies used in this study included mouse monoclonal antibody to HA (Roche), rabbit polyclonal antibody to HA (Covance), antibody to Myc (Upstate Biotechnology), antibody to β-catenin (Transduction Laboratories), antibody to γ-tubulin (Sigma), antibody to Flag (Sigma), antibody to Dvl2 (Abcam), antibody to polyubiquitin clone FK1 (Affiniti Research), and antibody to GFP (Santa Cruz Biotechnology). Rabbit polyclonal antiserum against Dvl was provided by S. Sokol.

Cell Culture and Western Blots. HEK 293T cells were grown in DMEM supplemented with 10% FBS. Transient transfections were performed by using the calcium phosphate method. To determine steady-state levels of proteins, HEK 293T cells were transfected in 10-cm dishes by the calcium phosphate method, harvested after 24 h in cold PBS, and lysed in a buffer containing 20 mM Tris·HCl (pH 7,5), 1% Triton X-100, 25 mM NaF, 12.5 mM $Na_4P_2O_7$, 0.1 mM EDTA, 50 mM NaCl, 2 mM Na_3VO_4, and protease inhibitors. To analyze the turnover of proteins, cells were treated with 40 μg/mL cycloheximide in DMEM 48 h after transfection; cells were lysed in the same buffer as above after 0, 2, 4, and 8 h of incubation with cycloheximide. To analyze cytoplasmic levels of β-catenin, transfected HEK 293T cells were treated as described (35). Proteins were fractionated by 10% SDS/PAGE, and protein levels were analyzed by Western blot.

Luciferase Assay. HEK 293T cells seeded in 12-cm dishes were transiently transfected with a luciferase reporter construct, a β-galactosidase expression vector, and vectors directing the expression of proteins as indicated. Cells were harvested 24 h after transfection in cold PBS and lysed in 100 μL of reporter lysis buffer (Applied Biosystems). Luciferase activity was determined by using a commercial assay system following the manufacturer's instructions and normalized to β-galactosidase activity to correct for transfection efficiency.

Ubiquitylation Assay. Thirty hours after transfection, HEK 293 T cells were washed in PBS and lysed in buffer A (8 M urea, 100 mM NaH_2PO_4, 10 mM Tris, and 1% Triton X-100, pH 8, all steps at room temperature). The supernatant obtained after two centrifugation steps was used for purification on Ni^{2+}–nitrilotriacetate agarose (Qiagen) for 1.5 h and washed twice with buffer A and twice with buffer B (same as A except for 0.5% Triton X-100 and pH 6.3). Bound proteins were eluted with buffer C (same as A except for 0.1% Triton X-100 and pH 4.5).

***Xenopus laevis* Embryo Manipulations.** The methods used have been described previously (11). Briefly, *Xenopus* females were injected with 600–800 units of human chorionic gonadotropin. Eggs were harvested, fertilized in vitro, and cultured in 0.3× Marc's modified Ringer's medium (MMR). Capped synthetic RNAs were generated by using the mMessage mMachine kit (Ambion). Plasmids were linearized and transcribed as follows: Centrin-RFP (NotI, SP6); CLAMP-GFP (NotI, SP6); xDvl2-GFP (KpnI, T3); GFP-HA (SalI, T7); hANAPC2-HA (SalI, T7). The RNA microinjections were performed according to standard techniques using a time- and pressure-triggered microinjection system (Narishige) at volumes of 8–10 nL per blastomere. The *Xenopus tropicalis* ANAPC2 orthologue was identified by BLAST search of the U.S. Department of Energy Joint Genome Institute (JGI) genome assembly 4.1 on scaffold 366. A 1-kb fragment was amplified by RT-PCR (Invitrogen) using *Xenopus laevis* mRNA. The PCR amplification of intron 2 from genomic DNA revealed the intron/exon boundaries. The sequences were deposited at the National Center for Biotechnology Information (accession No. EU887535) Splice-blocking MOs were obtained from Gene Tools: ANAPC2 I2E3 (Mo1), 5′-GTCACTAGAGAAATCCAA-GAAATAC-3′; ANAPC2 E2I2 (Mo2), 5′-TGCACCTAAAAACTACTTACAAA-3′; standard control, 5′-CCTCTTACCTCAGTTACAATTTATA-3′. Both MOs prevented splicing of intron 2 and introduced an in-frame termination codon, which was confirmed by RT-PCR and sequencing of the resulting product. To determine the polarity of basal bodies, embryos were fixed at stage 28–30. Confocal imaging was performed on an inverted Zeiss LSM 5 DUO Live. Angles were measured with ImageJ (http://rsbweb.nih.gov/ij/) and analyzed with Oriana 2.0 statistical software (Kovach Computing Service). For streamline assays, fluorescent beads (Molecular Probes/Invitrogen) were diluted in 0.3× MMR 1:1,000,000 and imaged in intervals of 0.1 s with a SPOT Insight FireWire system (Diagnostic Instruments) on a Leica MZ16 stereomicroscope. Video recordings were analyzed with Imaris 6.0 software (Bitplane). Approximately 50–300 beads were tracked, and the average speed was calculated for each embryo. Streamline images resulted from superimposing all frames of one recording. Confocal images of xDvl2-GFP (Fig. 5*D*) and mem-GFP (Fig. S3) were recorded on a Zeiss LSM 510 microscope. Four optical sections at the apical membrane were stacked to depict the entire apical cell surface. Single-channel images in Fig. 5*D* are magnifications of one optical focus plane containing basal bodies. Imaging settings were identical between control MO and ANAPC2 MO embryos. For preparation of *Xenopus* embryo lysates, 20 embryos for each group were injected as indicated and lysed at stage 10 with the same lysis buffer as described above. The supernatant obtained after two centrifugation steps at 17,000 × *g* was used to analyze protein levels by Western blot.

Respiratory Epithelial Cells. Human respiratory epithelial cells were obtained by nasal brush and incubated at 37 °C in serum-free bronchial epithelial growth medium (Clonetics and Lonza) as described (36). For staining, the specimen were fixed in 4% paraformaldehyde/PBS and blocked in 5% goat serum supplemented with 0.1% Triton X-100. Staining was done following standard procedures. Images were taken on a Zeiss Axiovert 200 M equipped with the Zeiss ApoTome technology using a 63 × 1.2 numerical aperture water-immersion objective. Images were processed with Axiovert software.

ACKNOWLEDGMENTS. We thank all members of G.W.'s laboratory for helpful discussions. This work was supported by grants from the National Institute of General Medical Sciences of the National Institutes of Health, Sandler Program for Asthma Research, and March of Dimes (to J.B.W.), Deutsche Krebshilfe (to J.G.), and European Union (EUCILIA) and Deutsche Forschungsgemeinschaft (to G.W.).

1. Klein TJ, Mlodzik M (2005) Planar cell polarization: An emerging model points in the right direction. *Annu Rev Cell Dev Biol* 21:155–176.
2. Wang Y, Nathans J (2007) Tissue/planar cell polarity in vertebrates: New insights and new questions. *Development* 134:647–658.
3. Wu J, Jenny A, Mirkovic I, Mlodzik M (2008) Frizzled–Dishevelled signaling specificity outcome can be modulated by Diego in *Drosophila*. *Mech Dev* 125:30–42.
4. Jenny A, Reynolds-Kenneally J, Das G, Burnett M, Mlodzik M (2005) Diego and Prickle regulate Frizzled planar cell polarity signaling by competing for Dishevelled binding. *Nat Cell Biol* 7:691–697.
5. Park TJ, Mitchell BJ, Abitua PB, Kintner C, Wallingford JB (2008) Dishevelled controls apical docking and planar polarization of basal bodies in ciliated epithelial cells. *Nat Genet* 40:871–879.
6. Miyazaki K, et al. (2004) NEDL1, a novel ubiquitin-protein isopeptide ligase for dishevelled-1, targets mutant superoxide dismutase-1. *J Biol Chem* 279:11327–11335.
7. Angers S, et al. (2006) The KLHL12–Cullin-3 ubiquitin ligase negatively regulates the Wnt–β-catenin pathway by targeting Dishevelled for degradation. *Nat Cell Biol* 8:348–357.
8. Creyghton MP, et al. (2005) PR72, a novel regulator of Wnt signaling required for Naked cuticle function. *Genes Dev* 19:376–386.
9. Chan DW, Chan CY, Yam JW, Ching YP, Ng IO (2006) Prickle-1 negatively regulates Wnt/β-catenin pathway by promoting Dishevelled ubiquitination/degradation in liver cancer. *Gastroenterology* 131:1218–1227.
10. Zhang L, Gao X, Wen J, Ning Y, Chen YG (2006) Dapper 1 antagonizes Wnt signaling by promoting Dishevelled degradation. *J Biol Chem* 281:8607–8612.
11. Simons M, et al. (2005) Inversin, the gene product mutated in nephronophthisis type II, functions as a molecular switch between Wnt signaling pathways. *Nat Genet* 37:537–543.
12. Morgan D, et al. (2002) Expression analyses and interaction with the anaphase promoting complex protein Apc2 suggest a role for inversin in primary cilia and involvement in the cell cycle. *Hum Mol Genet* 11:3345–3350.
13. Peters JM (2006) The anaphase promoting complex/cyclosome: A machine designed to destroy. *Nat Rev Mol Cell Biol* 7:644–656.
14. Musacchio A, Salmon ED (2007) The spindle-assembly checkpoint in space and time. *Nat Rev Mol Cell Biol* 8:379–393.
15. Pesin JA, Orr-Weaver TL (2008) Regulation of APC/C activators in mitosis and meiosis. *Annu Rev Cell Dev Biol* 24:475–499.
16. Harper JW, Burton JL, Solomon MJ (2002) The anaphase-promoting complex: It's not just for mitosis any more. *Genes Dev* 16:2179–2206.

17. Konishi Y, Stegmuller J, Matsuda T, Bonni S, Bonni A (2004) Cdh1–APC controls axonal growth and patterning in the mammalian brain. *Science* 303:1026–1030.
18. Juo P, Kaplan JM (2004) The anaphase-promoting complex regulates the abundance of GLR-1 glutamate receptors in the ventral nerve cord of *C. elegans*. *Curr Biol* 14:2057–2062.
19. van Roessel P, Elliott DA, Robinson IM, Prokop A, Brand AH (2004) Independent regulation of synaptic size and activity by the anaphase-promoting complex. *Cell* 119:707–718.
20. Rappleye CA, Tagawa A, Lyczak R, Bowerman B, Aroian RV (2002) The anaphase-promoting complex and separin are required for embryonic anterior–posterior axis formation. *Dev Cell* 2:195–206.
21. Slack C, Overton PM, Tuxworth RI, Chia W (2007) Asymmetric localization of Miranda and its cargo proteins during neuroblast division requires the anaphase-promoting complex/cyclosome. *Development* 134:3781–3787.
22. Schmidt A, et al. (2005) *Xenopus* polo-like kinase Plx1 regulates XErp1, a novel inhibitor of APC/C activity. *Genes Dev* 19:502–513.
23. Hershko A, Ciechanover A (1998) The ubiquitin system. *Annu Rev Biochem* 67:425–479.
24. Axelrod JD, Miller JR, Shulman JM, Moon RT, Perrimon N (1998) Differential recruitment of Dishevelled provides signaling specificity in the planar cell polarity and Wingless signaling pathways. *Genes Dev* 12:2610–2622.
25. Boutros M, Paricio N, Strutt DI, Mlodzik M (1998) Dishevelled activates JNK and discriminates between JNK pathways in planar polarity and wingless signaling. *Cell* 94:109–118.
26. Axelrod JD (2001) Unipolar membrane association of Dishevelled mediates Frizzled planar cell polarity signaling. *Genes Dev* 15:1182–1187.
27. Penton A, Wodarz A, Nusse R (2002) A mutational analysis of Dishevelled in *Drosophila* defines novel domains in the Dishevelled protein and novel suppressing alleles of axin. *Genetics* 161:747–762.
28. Moody SA (1987) Fates of the blastomeres of the 16-cell stage *Xenopus* embryo. *Dev Biol* 119:560–578.
29. Park TJ, Gray RS, Sato A, Habas R, Wallingford JB (2005) Subcellular localization and signaling properties of Dishevelled in developing vertebrate embryos. *Curr Biol* 15:1039–1044.
30. Dube P, et al. (2005) Localization of the coactivator Cdh1 and the cullin subunit Apc2 in a cryo-electron microscopy model of vertebrate APC/C. *Mol Cell* 20:867–879.
31. Vodermaier HC, Gieffers C, Maurer-Stroh S, Eisenhaber F, Peters JM (2003) TPR subunits of the anaphase-promoting complex mediate binding to the activator protein CDH1. *Curr Biol* 13:1459–1468.
32. Thornton BR, et al. (2006) An architectural map of the anaphase-promoting complex. *Genes Dev* 20:449–460.
33. Tugendreich S, Tomkiel J, Earnshaw W, Hieter P (1995) CDC27Hs colocalizes with CDC16Hs to the centrosome and mitotic spindle and is essential for the metaphase to anaphase transition. *Cell* 81:261–268.
34. Mitchell B, Jacobs R, Li J, Chien S, Kintner C (2007) A positive feedback mechanism governs the polarity and motion of motile cilia. *Nature* 447:97–101.
35. Kim E, et al. (1999) The polycystic kidney disease 1 gene product modulates Wnt signaling. *J Biol Chem* 274:4947–4953.
36. Fliegauf M, et al. (2006) Nephrocystin specifically localizes to the transition zone of renal and respiratory cilia and photoreceptor connecting cilia. *J Am Soc Nephrol* 17:2424–2433.